Controlling Nonsequential Double Ionization in Two-Color Circularly Polarized Femtosecond Laser Fields

Christopher A. Mancuso,[1,*] Kevin M. Dorney,[1] Daniel D. Hickstein,[1] Jan L. Chaloupka,[2] Jennifer L. Ellis,[1] Franklin J. Dollar,[1,†] Ronny Knut,[1,‡] Patrik Grychtol,[1] Dmitriy Zusin,[1] Christian Gentry,[1] Maithreyi Gopalakrishnan,[1] Henry C. Kapteyn,[1] and Margaret M. Murnane[1]

[1]*JILA, Department of Physics, University of Colorado and NIST, Boulder, Colorado 80309, USA*

[2]*Department of Physics and Astronomy, University of Northern Colorado, Greeley, Colorado 80639, USA*

(Received 21 April 2016; revised manuscript received 28 June 2016; published 20 September 2016)

Atoms undergoing strong-field ionization in two-color circularly polarized femtosecond laser fields exhibit unique two-dimensional photoelectron trajectories and can emit bright circularly polarized extreme ultraviolet and soft-x-ray beams. In this Letter, we present the first experimental observation of nonsequential double ionization in these tailored laser fields. Moreover, we can enhance or suppress nonsequential double ionization by changing the intensity ratio and helicity of the two driving laser fields to maximize or minimize high-energy electron-ion rescattering. Our experimental results are explained through classical simulations, which also provide insight into how to optimize the generation of circularly polarized high harmonic beams.

DOI: 10.1103/PhysRevLett.117.133201

When a strong laser field ($\sim 10^{14}$–10^{16} W cm^{-2}) interacts with an atom or molecule, an electron can be liberated via tunnel ionization, accelerated in the laser field, and driven back to the parent ion [1–4]. The interaction of the field-driven electron wave packet with its parent ion can lead to several outcomes. In some cases, the electron can recombine with the parent ion, releasing a series of attosecond bursts of high-energy photons through the process of high harmonic generation (HHG) [1–6]. This process has been shown to produce photon energies ranging from the extreme ultraviolet (EUV) to soft x rays (>1 keV [7]). HHG beams in the EUV region have been used to understand a wide range of processes, including the ultrafast dynamics of electronic or magnetic states [8–12], nanoscale heat transport [13], and the spatial resolution limits of light-based imaging [14–18]. If the field-driven electron does not recombine to produce HHG, it can alternatively rescatter off the parent ion. These rescattered electrons can encode atomic and molecular structural information about the parent ion with subangstrom spatial resolution and attosecond temporal resolution [19–21]. Finally, the field-driven electron may recollide with the parent ion, leading to a second electron being ionized through the process of nonsequential double ionization (NSDI) [22,23]. Recently, NSDI driven by linearly polarized laser fields has been used to provide insight into correlated electron dynamics [24,25].

To study HHG, electron-ion rescattering, and NSDI, linearly polarized laser fields are typically used to drive strong-field ionization and the resulting rescattering processes. The preference for linear fields is due to the fact that one-color circularly polarized laser fields do not efficiently drive the electron back to the parent ion, so that rescattering processes are significantly suppressed [26–28]. However, it was theoretically proposed and recently experimentally demonstrated that two-color counter-rotating circularly polarized laser fields can be used to drive the HHG process and generate circularly polarized EUV [29–34] and soft-x-ray beams [35] bright enough for applications, such as performing the first tabletop x-ray circular dichroism measurements [33,35], using high harmonic spectroscopy to measure the orbital angular momentum symmetry of atomic orbitals [36], and three-dimensional attosecond meteorology [37].

Recently, photoelectron spectroscopy was used to experimentally observe electron-ion rescattering in these fields [38,39]. The fact that electrons travel along two-dimensional (2D) trajectories before returning to the parent ion [40,41] allows for the tunnel-ionization process and electron-ion rescattering process to occur at different angles, making it easier to deconvolve the atomic and molecular structural information encoded by the rescattered electrons. The trajectories of the electrons can be steered (by changing the relative intensity ratio between the two laser fields), providing new probes of atomic and molecular dynamics.

In this Letter, we make the first experimental observation of NSDI in two-color circularly polarized laser fields, providing new insights into electron dynamics in such fields. We find that we can control NSDI by changing the intensity ratio and helicity of the two driving laser fields, where counter-rotating fields significantly enhance NSDI while co-rotating fields suppress it. Moreover, we can enhance NSDI in counter-rotating fields further by changing the intensity ratio of the two fields to maximize high-energy electron-ion rescattering. To qualitatively describe our experimental results, we employ classical ensemble (CE) simulations [42–47], which capture two-electron

dynamics. Additionally, we consider single-electron dynamics within the tunneling approximation via classical trajectory Monte Carlo (CTMC) simulations [39] since they provide intuitive explanations of the underlying mechanisms of NSDI in two-color circularly polarized fields. These calculations confirm that the returning electron energy spectrum can be varied significantly by changing the relative intensity ratio between the two laser fields, where NSDI is maximized for a ratio of the intensity of the second harmonic ("blue") beam to the intensity of the fundamental ("red") beam (I_B/I_R) of ≈ 3. Finally, the returning electron energy spectrum in two-color counter-rotating fields exhibits a narrower bandwidth than that of a linearly polarized field at the fundamental frequency and also exhibits a tunable cutoff energy. Thus, HHG driven by two-color counter-rotating fields can generate a unique quasimonochromatic light source with tunable photon energy.

NSDI in one-color linearly polarized fields has generated great interest for studying correlated electron dynamics [24,25]. However, under these conditions, the electron is driven in a 1D straight-line trajectory, so although NSDI can be observed, there exist limited ways to control the process [48,49]. Observations of NSDI have been reported in one-color elliptically polarized fields [50] and in one-color circularly polarized fields in atoms with extremely low ionization energies [51], but the yields are significantly lower than with linear polarization. Likewise, HHG and high-energy electron-ion rescattering are significantly suppressed in these fields [26–28]. Since HHG and high-energy electron-ion rescattering can occur efficiently in two-color circularly polarized fields [32,33,38], these fields offer the optimum route to generate NSDI with electrons that are driven in 2D trajectories before recolliding with the parent ion. Additionally, two-color circularly polarized fields also offer the best route for controlling NSDI, as the 2D electron trajectories can be steered simply by changing the intensity and ellipticity of the driving laser fields.

In addition to providing a route for controlling NSDI using two-color circularly polarized fields, the results presented here help to expand our understanding of the single-atom physics behind HHG. While HHG emission can provide insight into the single-atom physics, experimentally measured HHG spectra are often convolved with the macroscopic phase-matching physics needed to generate bright beams [52,53]. Similarly, photoelectron spectroscopy is a useful tool for studying single-atom physics [39,54], but the vast majority of electrons do not rescatter off the parent ion, making it difficult to detect those that do. In contrast, NSDI corresponds exclusively to hard rescattered electrons and is intrinsically a single-atom process. Therefore, NSDI provides clear and direct insight into the fundamental rescattering physics that underlies HHG.

To study NSDI in two-color circularly polarized fields, we used the fundamental (790 nm, 40 fs) and second harmonic (395 nm) of a Ti:sapphire regenerative amplifier (KMLabs Wyvern HP) [Fig. 1(a)]. We temporally overlapped the two pulses with a Mach-Zehnder interferometer and independently controlled the intensity and polarization of each beam. The pulses were then focused onto a skimmed supersonic jet of argon gas, and the resulting ion signal was recorded using a time-of-flight spectrometer [see the Supplemental Material (SM [55])]. Each time-of-flight spectrum consists of 10^5 laser shots. The single- and double-ionization yields were experimentally recorded as a function of the total intensity. We varied both the I_B/I_R ratio and the relative helicity (i.e., counter- and co-rotating fields), which changes the shape of the combined electric field and electron trajectory [Fig. 1(b)]. In counter-rotating fields, an electron can be efficiently driven back to the parent ion in 2D trajectories, whereas it is much harder for an electron to return to the parent ion in co-rotating fields (see the SM).

For all I_B/I_R ratios and both helicities, the Ar^{1+} yields as a function of total intensity remain the same (Fig. 2). This is expected because to first order, the tunnel-ionization rate [56] depends only on the electric field strength and not the frequency. However, the significant differences in Ar^{2+} yields for different I_B/I_R ratios and helicities allow us to identify the presence of NSDI.

For the co-rotating cases, the Ar^{2+} yields are the same for all intensity ratios, and the Ar^{2+} signal only becomes appreciable after the Ar^{1+} yield has saturated, indicating that the intensity is high enough such that sequential ionization is the dominant double-ionization mechanism. Conversely,

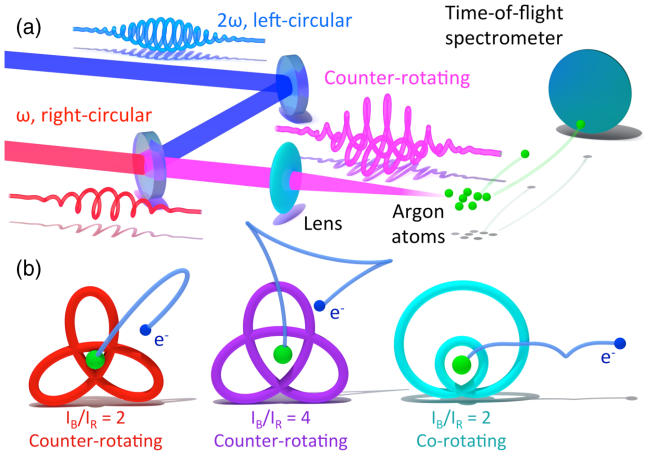

FIG. 1. (a) The experimental scheme used to study nonsequential double ionization in two-color (ω, 2ω) circularly polarized fields. The apparatus consists of a femtosecond laser system, a Mach-Zehnder interferometer, and a time-of-flight spectrometer. (b) The electric fields for two-color counter-rotating fields for I_B/I_R ratios of 2 (left-hand thick red curve) and 4 (middle thick purple curve) and for a co-rotating field at an I_B/I_R ratio of 2 (right-hand thick cyan curve). Counter-rotating fields can efficiently drive electrons (small blue spheres) back to the parent ion (large green spheres) in 2D trajectories, whereas it is much harder for an electron to return to the parent ion in co-rotating fields.

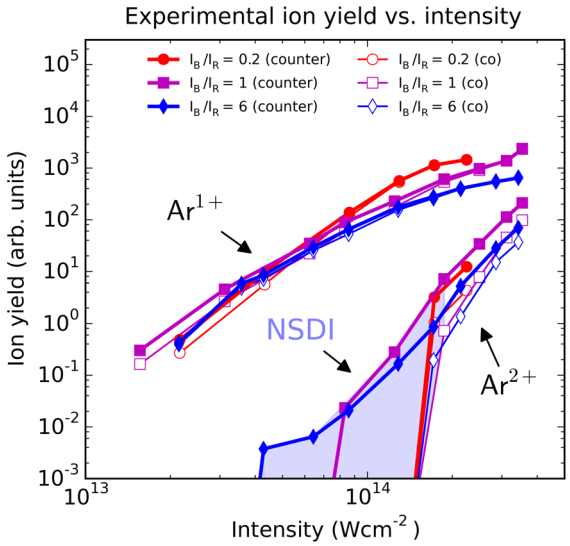

FIG. 2. Experimentally measured single- and double-ionization yields in argon for two-color circularly polarized fields. The fields are combined as either counter-rotating (filled symbols) or co-rotating (open symbols) fields and with three different ratios of the second harmonic intensity to the intensity of the fundamental I_B/I_R: 0.2 (circles), 1 (squares), and 6 (diamonds). NSDI (shaded region) is observed in counter-rotating fields when the I_B/I_R ratio is 1 and 6. However, NSDI is not observed for co-rotating fields or for the counter-rotating case of $I_B/I_R = 0.2$. Note: The intensities were slightly rescaled relative to their estimated values in order to provide comparable single-ionization yields (see the SM).

for the counter-rotating case, the Ar^{2+} yield is dependent on the I_B/I_R ratio. For I_B/I_R ratios of 1 and 6, a significant amount of the Ar^{2+} signal can be seen below the Ar^{1+} saturation intensity. However, when the I_B/I_R ratio is 0.2, the Ar^{2+} yield is nearly identical to that of the co-rotating cases, suggesting that NSDI is strongly suppressed when the I_B/I_R ratio decreases below a certain value.

To provide qualitative theoretical support to our experimental findings, we used the CE method [42–45,57,58] to simulate single- and double-ionization yields in an argonlike atom (Fig. 3). In our CE model, an ensemble of 2×10^4 atoms with randomized initial electron positions and momenta is generated. The atoms are then placed under the influence of a strong laser field, and the resulting ion signal is recorded (see the SM). In our simulations, the peak of the electric field amplitude is held fixed for a given set of simulations, as the field amplitude is the relevant parameter for determining ionization probability.

The simulated ionization yields agree with our experimental results [Fig. 3(a)]. First, the CE simulations predict that NSDI is significantly suppressed in co-rotating fields, as is expected since co-rotating fields do not efficiently drive electrons back to the parent ion (see the SM). However, a small amount of NSDI can be seen for the co-rotating case of $I_B/I_R = 6$. The yield is sufficiently low enough that it cannot be detected in our experiment, but the observation in the simulation agrees with the experimental observation of HHG in co-rotating fields, albeit with significantly lower flux than with counter-rotating fields [29]. Second, the Ar^{2+} yields from counter-rotating fields strongly depend on the I_B/I_R ratio. Similar to the experimental results, NSDI is prominent in counter-rotating fields when the I_B/I_R ratio is 1 and 6, but little NSDI occurs when the I_B/I_R ratio is 0.2.

To understand how the intensity ratio affects NSDI, we performed the CE simulations for a range of I_B/I_R ratios but kept the total electric field amplitude fixed, corresponding to a one-color linearly polarized field at 5×10^{14} W cm^{-2} [Fig. 3(b)]. The intensity of 5×10^{14} W cm^{-2} is chosen as this corresponds to the middle of the NSDI "knee" [22]. The results of the CE simulations [Fig. 3(b)] show that NSDI occurs over a broad range of I_B/I_R ratios and the NSDI yield optimizes at $I_B/I_R \approx 2$. One noticeable feature is that the Ar^{2+} yield is not symmetric and a "plateau" is formed that extends to $I_B/I_R \approx 15$. The CE simulations were recently used to perform an in-depth theoretical study of NSDI in two-color circularly polarized laser fields in helium [58], looking at the electron energy spectra, momenta, ionization

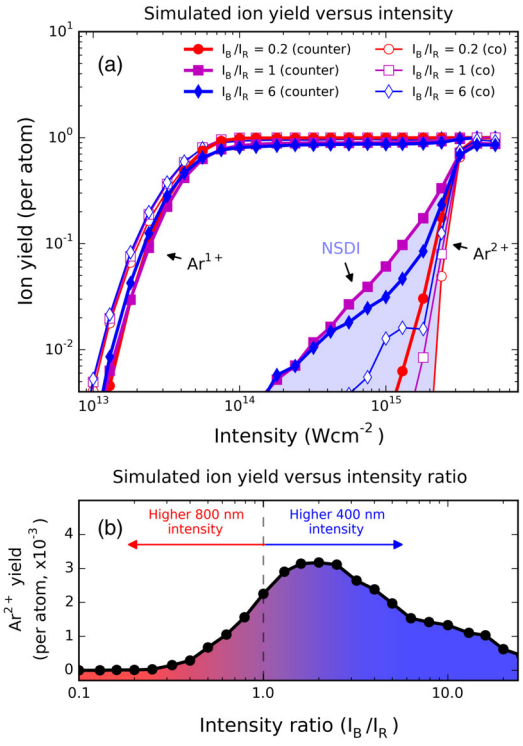

FIG. 3. Simulated single- and double-ionization yields in argon using a classical ensemble model. (a) A significant amount of NSDI (shaded region) occurs in counter-rotating fields when the I_B/I_R ratio is 1 and 6 and is suppressed in the co-rotating cases and the counter-rotating case when $I_B/I_R = 0.2$. (b) The double-ionization yield of argon at 5×10^{14} W cm^{-2} is comprised entirely of NSDI and shows that NSDI occurs over a broad range of I_B/I_R ratios. The Ar^{2+} yield is optimized at $I_B/I_R \approx 2$.

timing, sample trajectories, and a comparison to a one-color 800-nm field.

The dependence of NSDI on the I_B/I_R ratio can also be understood by looking at the energy of electrons as they return to the parent ion (Fig. 4). We calculate the kinetic energy spectra of the returning electrons using one-active-electron CTMC simulations [39] within the tunnel-ionization approximation (see the SM). We consider an electron "returned" if it approaches within 0.05 nm (~1 Bohr radius) of the parent ion. Of course, this approach provides only a relative measure of rescattering rates, and not the rates themselves, which will be significantly lower. As in the CE simulations, the total electric field amplitude is kept fixed, corresponding to a one-color linearly polarized field at 5×10^{14} W cm^{-2}, and each spectrum consists of 5×10^4 electron trajectories.

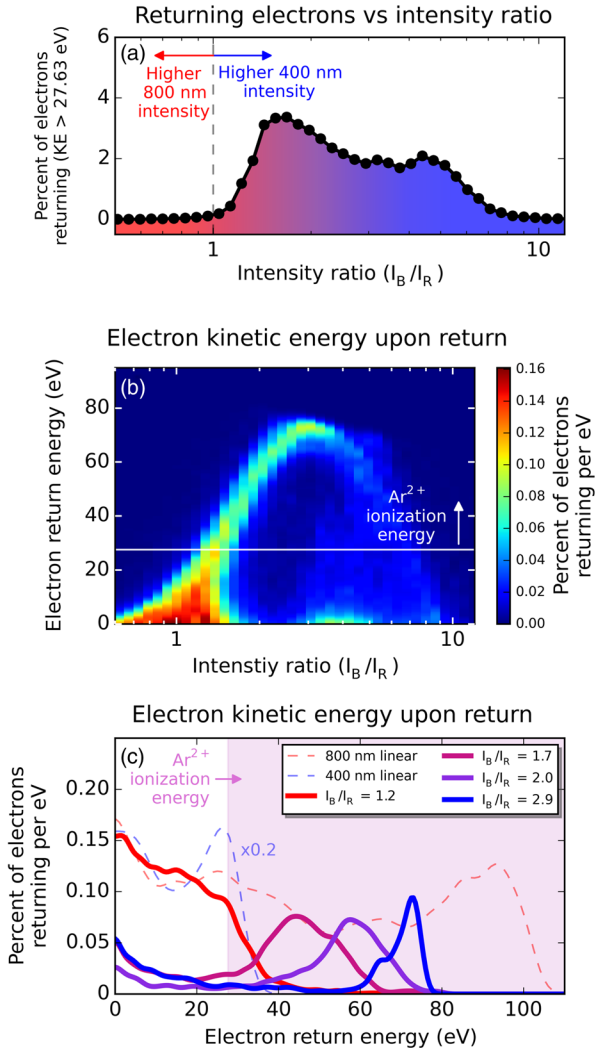

FIG. 4. Classical trajectory Monte Carlo simulations show the yield of electrons that return within 0.05 nm of the parent ion, and the energy of the electrons at the moment of return. (a) The percent of electrons that return to the parent ion with a kinetic energy (KE) that is greater than the second ionization energy of argon (27.63 eV) gives an estimate of NSDI and agrees well with the classical ensemble model [Fig. 3(b)]. (b) The cutoff energy of the returning electrons strongly depends on the I_B/I_R ratio. (c) The returning energy spectrum of electrons in two-color counter-rotating fields exhibits a narrower bandwidth than that of a linearly polarized field at the fundamental frequency, allowing for the generation of a quasimonochromatic EUV light source with a tunable photon energy.

The CTMC simulations provide an estimate of the NSDI yield, which can be inferred by the percent of electrons that return to the parent ion with kinetic energies in excess of the second ionization potential of argon (27.63 eV) [Fig. 4(a)]. The CTMC simulations agree well with the CE model, showing that at an intensity of 5×10^{14} W cm^{-2} in argon, NSDI peaks when $I_B/I_R \approx 1.5$, and a plateau is formed that extends to $I_B/I_R \approx 7$. At I_B/I_R ratios less than 1.5, a large percentage of electrons is driven back to the parent atom with energies below the ionization energy of Ar^{2+} (27.63 eV) [Fig. 4(b)], showing that recollision excitation with subsequent ionization may play an important role in NSDI at these low I_B/I_R ratios. This may explain the difference in NSDI yield between the CE and CTMC models at these low I_B/I_R ratios [see Figs. 3(b) and 4(a)], as the CE model includes the recollision excitation with subsequent ionization mechanism.

The kinetic energy spectra of the returning electrons can also inform how the intensity ratio of the two-color driving field can be used to control the rescattering process. When a linearly polarized field is used to drive the rescattering process, the resulting returning energy spectrum consists of a plateau followed by an abrupt cutoff [1] [Fig. 4(c)]. However, the results of the CTMC simulations show that in two-color circularly polarized laser fields, the returning energy spectrum can be varied significantly by changing the I_B/I_R ratio [Fig. 4(b)]. The cutoff energy is driven to a maximum when $I_B/I_R \approx 3$, which is close to the I_B/I_R ratio that was found to optimize high-energy electron-ion rescattering in Ref. [39]. In general, the returning energy spectrum of electrons in two-color counter-rotating fields exhibits a narrower bandwidth than that of a linearly polarized field at the fundamental frequency, but with a tunable cutoff energy that can be set to reach nearly the same maximum as seen from the fundamental field alone. This shows that HHG driven by two-color counter-rotating fields can allow for the generation of a quasimonochromatic EUV light source with tunable photon energy.

In conclusion, we have made the first experimental observation of NSDI in two-color circularly polarized laser fields. We showed the NSDI process can be controlled by significantly suppressing NSDI in co-rotating fields and enhancing NSDI in counter-rotating fields by changing the intensity ratio of the two-color fields. We confirmed our experimental results using classical simulations, showing that the yield of electrons that return to the parent ion and the electron's kinetic energy upon return can explain the dependence of NSDI on the two-color laser field intensity

ratio. These findings help inform the single-atom picture of HHG driven by these fields, showing the possibility of generating a quasimonochromatic EUV light source with a tunable photon energy. Additionally, since electrons in two-color circularly polarized fields can be driven in two-dimensional trajectories before returning to the parent ion, electron-electron correlation experiments in these fields could serve as a new tool in studying ultrafast molecular dynamics.

This research was primarily supported by the Department of Energy Office Basic Energy Sciences Grant No. DE-FG02-99ER14982. We also acknowledge support from the Department of Energy Office Basic Energy Sciences X-Ray Scattering Program Grant No. DE-SC0002002 that provided the optical setup used in this work. J. E. and C. M. acknowledge support from National Science Foundation (DGE-1144083).

M. M. and H. K. have a financial interest in KMLabs.

Note added in the proof—We note that a completely independent experimental confirmation of NSDI in counter-rotating fields has recently been completed using an electron-ion coincidence spectrometer [59].

*christopher.mancuso@colorado.edu

†Present address: Department of Physics and Astronomy, University of California, Irvine, CA 92697, USA.

‡Present address: Department of Physics and Astronomy, University of Uppsala, Uppsala SE-571 20, Sweden.

[1] A. Mcpherson, G. Gibson, H. Jara, U. Johann, T. S. Luk, I. A. McIntyre, K. Boyer, and C. K. Rhodes, J. Opt. Soc. Am. B **4**, 595 (1987).

[2] M. Ferray, A. L'Huillier, X. F. Li, L. A. Lompre, G. Mainfray, and C. Manus, J. Phys. B **21**, L31 (1988).

[3] M. Y. Kuchiev, Pis'ma Zh. Eksp. Teor. Fiz. **45**, 319 (1987) [JETP Lett. **45**, 404 (1987)].

[4] J. L. Krause, K. J. Schafer, and K. C. Kulander, Phys. Rev. Lett. **68**, 3535 (1992).

[5] M.-C. Chen, C. Mancuso, C. Hernandez-Garcia, F. Dollar, B. Galloway, D. Popmintchev, P.-C. Huang, B. Walker, L. Plaja, A. A. Jaro-Becker, A. Becker, M. M. Murnane, H. C. Kapteyn, and T. Popmintchev, Proc. Natl. Acad. Sci. U.S.A. **111**, E2361 (2014).

[6] D. Popmintchev, C. Hernandez-Garcia, F. Dollar, C. Mancuso, J. A. Perez-Hernandez, M.-C. Chen, A. Hankla, X. Gao, B. Shim, A. L. Gaeta, M. Tarazkar, D. A. Romanov, R. J. Levis, J. A. Gaffney, M. Foord, S. B. Libby, A. Jaron-Becker, A. Becker, L. Plaja, M. M. Murnane, H. C. Kapteyn, and T. Popmintchev, Science **350**, 1225 (2015).

[7] T. Popmintchev, M.-C. Chen, D. Popmintchev, P. Arpin, S. Brown, S. Alisauskas, G. Andriukaitis, T. Balciunas, O. D. Mucke, A. Pugzlys, A. Baltuska, B. Shim, S. E. Schrauth, A. Gaeta, C. Hernandez-Garcia, L. Plaja, A. Becker, A. Jaron-Becker, M. M. Murnane, and H. C. Kapteyn, Science **336**, 1287 (2012).

[8] E. Turgut, C. La-o-vorakiat, J. M. Shaw, P. Grychtol, H. T. Nembach, D. Rudolf, R. Adam, M. Aeschlimann, C. M. Schneider, T. J. Silva, M. M. Murnane, H. C. Kapteyn, and S. Mathias, Phys. Rev. Lett. **110**, 197201 (2013).

[9] S. Hellmann, T. Rohwer, M. Kalläne, K. Hanff, C. Sohrt, A. Stange, A. Carr, M. M. Murnane, H. C. Kapteyn, L. Kipp, M. Bauer, and K. Rossnagel, Nat. Commun. **3**, 1069 (2012).

[10] E. Goulielmakis, Z.-H. Loh, A. Wirth, R. Santra, N. Rohringer, V. S. Yakovlev, S. Zherebtsov, T. Pfeifer, A. M. Azzeer, M. F. Kling, S. R. Leone, and F. Krausz, Nature (London) **466**, 739 (2010).

[11] E. R. Hosler and S. R. Leone, Phys. Rev. A **88**, 023420 (2013).

[12] P. Matyba, A. Carr, C. Chen, D. L. Miller, G. Peng, S. Mathias, M. Mavrikakis, D. S. Dessau, M. W. Keller, H. C. Kapteyn, and M. Murnane, Phys. Rev. B **92**, 041407 (2015).

[13] K. M. Hoogeboom-Pot, J. N. Hernandez-Charpak, X. Gu, T. D. Frazer, E. H. Anderson, W. Chao, R. W. Falcone, R. Yang, M. M. Murnane, H. C. Kapteyn, and D. Nardi, Proc. Natl. Acad. Sci. U.S.A. **112**, 4846 (2015).

[14] B. Zhang, D. F. Gardner, M. D. Seaberg, E. R. Shanblatt, H. C. Kapteyn, M. M. Murnane, and D. E. Adams, Ultramicroscopy **158**, 98 (2015).

[15] M. D. Seaberg, B. Zhang, D. F. Gardner, E. R. Shanblatt, M. M. Murnane, H. C. Kapteyn, and D. E. Adams, Optica **1**, 39 (2014).

[16] B. Zhang, M. D. Seaberg, D. E. Adams, D. F. Gardner, E. R. Shanblatt, J. M. Shaw, W. Chao, E. M. Gullikson, F. Salmassi, H. C. Kapteyn, and M. M. Murnane, Opt. Express **21**, 21970 (2013).

[17] R. A. Dilanian, B. Chen, G. J. Williams, H. M. Quiney, K. A. Nugent, S. Teichmann, P. Hannaford, L. V. Dao, and A. G. Peele, J. Appl. Phys. **106**, 023110 (2009).

[18] M. Zürch, C. Kern, and C. Spielmann, Opt. Express **21**, 21131 (2013).

[19] M. G. Pullen, B. Wolter, A.-T. Le, M. Baudisch, M. Hemmer, A. Senftleben, C. D. Schröter, J. Ullrich, R. Moshammer, C. D. Lin, and J. Biegert, Nat. Commun. **6**, 7262 (2015).

[20] J. Xu, C. I. Blaga, K. Zhang, Y. H. Lai, C. D. Lin, T. A. Miller, P. Agostini, and L. F. DiMauro, Nat. Commun. **5**, 4635 (2014).

[21] C. I. Blaga, J. Xu, A. D. DiChiara, E. Sistrunk, K. Zhang, P. Agostini, T. A. Miller, L. F. DiMauro, and C. D. Lin, Nature (London) **483**, 194 (2012).

[22] B. Walker, B. Sheehy, L. F. DiMauro, P. Agostini, K. J. Schafer, and K. C. Kulander, Phys. Rev. Lett. **73**, 1227 (1994).

[23] S. Larochelle, A. Talebpour, and S. L. Chin, J. Phys. B **31**, 1201 (1998).

[24] B. Bergues, M. Kübel, N. G. Johnson, B. Fischer, N. Camus, K. J. Betsch, O. Herrwerth, A. Senftleben, A. M. Sayler, T. Rathje, T. Pfeifer, I. Ben-Itzhak, R. R. Jones, G. G. Paulus, F. Krausz, R. Moshammer, J. Ullrich, and M. F. Kling, Nat. Commun. **3**, 813 (2012).

[25] C. F. de Morisson Faria and X. Liu, J. Mod. Opt. **58**, 1076 (2011).

[26] P. Dietrich, N. H. Burnett, M. Ivanov, and P. B. Corkum, Phys. Rev. A **50**, R3585 (1994).

[27] W. Becker, F. Grasbon, R. Kopold, D. B. Milošević, G. G. Paulus, and H. Walther, Adv. At. Mol. Opt. Phys. **48**, 35 (2002).
[28] W. A. Bryan, S. L. Stebbings, J. McKenna, E. M. L. English, M. Suresh, J. Wood, B. Srigengan, I. C. E. Turcu, J. M. Smith, E. J. Divall, C. J. Hooker, A. J. Langley, J. L. Collier, I. D. Williams, and W. R. Newell, Nat. Phys. **2**, 379 (2006).
[29] H. Eichmann, A. Egbert, S. Nolte, C. Momma, B. Wellegehausen, W. Becker, S. Long, and J. K. McIver, Phys. Rev. A **51**, R3414(R) (1995).
[30] S. Long, W. Becker, and J. K. McIver, Phys. Rev. A **52**, 2262 (1995).
[31] D. B. Milošević and W. Becker, Phys. Rev. A **62**, 011403(R) (2000).
[32] A. Fleischer, O. Kfir, T. Diskin, P. Sidorenko, and O. Cohen, Nat. Photonics **8**, 543 (2014).
[33] O. Kfir, P. Grychtol, E. Turgut, R. Knut, D. Zusin, D. Popmintchev, T. Popmintchev, H. Nembach, J. M. Shaw, A. Fleischer, H. Kapteyn, M. Murnane, and O. Cohen, Nat. Photonics **9**, 99 (2015).
[34] D. D. Hickstein, F. J. Dollar, P. Grychtol, J. L. Ellis, R. Knut, C. Hernández-García, D. Zusin, C. Gentry, J. M. Shaw, T. Fan, K. M. Dorney, A. Becker, A. Jaroń-Becker, H. C. Kapteyn, M. M. Murnane, and C. G. Durfee, Nat. Photonics **9**, 743 (2015).
[35] T. Fan, P. Grychtol, R. Knut, C. Hernández-García, D. D. Hickstein, D. Zusin, C. Gentry, F. J. Dollar, C. A. Mancuso, C. W. Hogle, O. Kfir, D. Legut, K. Carva, J. L. Ellis, K. M. Dorney, C. Chen, O. G. Shpyrko, E. E. Fullerton, O. Cohen, P. M. Oppeneer, D. B. Milošević, A. Becker, A. A. Jaroń-Becker, T. Popmintchev, M. M. Murnane, and H. C. Kapteyn, Proc. Natl. Acad. Sci. U.S.A. **112**, 14206 (2015).
[36] D. Baykusheva, M. S. Ahsan, N. Lin, and H. J. Wörner, Phys. Rev. Lett. **116**, 123001 (2016).
[37] C. Chen, Z. Tao, C. Hernández-García, P. Matyba, A. Carr, R. Knut, O. Kfir, D. Zusin, C. Gentry, P. Grychtol, O. Cohen, L. Plaja, A. Becker, A. Jaron-Becker, H. Kapteyn, and M. Murnane, Sci. Adv. **2**, e1501333 (2016).
[38] C. A. Mancuso, D. D. Hickstein, P. Grychtol, R. Knut, O. Kfir, X.-M. Tong, F. Dollar, D. Zusin, M. Gopalakrishnan, C. Gentry, E. Turgut, J. L. Ellis, M.-C. Chen, A. Fleischer, O. Cohen, H. C. Kapteyn, and M. M. Murnane, Phys. Rev. A **91**, 031402 (2015).
[39] C. A. Mancuso, D. D. Hickstein, K. M. Dorney, J. L. Ellis, E. Hasović, R. Knut, P. Grychtol, C. Gentry, M. Gopalakrishnan, D. Zusin, F. J. Dollar, X.-M. Tong, D. B. Milošević, W. Becker, H. C. Kapteyn, and M. M. Murnane, Phys. Rev. A **93**, 053406 (2016).
[40] E. Hasović, W. Becker, and D. B. Milošević, Opt. Express **24**, 6413 (2016).
[41] D. B. Milošević, Phys. Rev. A **93**, 051402(R) (2016).
[42] R. Panfili, S. L. Haan, and J. H. Eberly, Phys. Rev. Lett. **89**, 113001 (2002).
[43] P. J. Ho, R. Panfili, S. L. Haan, and J. H. Eberly, Phys. Rev. Lett. **94**, 093002 (2005).
[44] S. L. Haan, L. Breen, A. Karim, and J. H. Eberly, Phys. Rev. Lett. **97**, 103008 (2006).
[45] S. L. Haan, J. S. Van Dyke, and Z. S. Smith, Phys. Rev. Lett. **101**, 113001 (2008).
[46] J. Javanainen, J. H. Eberly, and Q. Su, Phys. Rev. A **38**, 3430 (1988).
[47] D. Bauer, Phys. Rev. A **56**, 3028 (1997).
[48] A. S. Alnaser, D. Comtois, A. T. Hasan, D. M. Villeneuve, J.-C. Kieffer, and I. V Litvinyuk, J. Phys. B **41**, 031001 (2008).
[49] A. Kamor, F. Mauger, C. Chandre, and T. Uzer, Phys. Rev. E **83**, 036211 (2011).
[50] S. Ben, T. Wang, T. Xu, J. Guo, and X. Liu, Opt. Express **24**, 7525 (2016).
[51] G. D. Gillen, M. A. Walker, and L. D. Van Woerkom, Phys. Rev. A **64**, 043413 (2001).
[52] T. Popmintchev, M.-C. Chen, P. Arpin, M. M. Murnane, and H. C. Kapteyn, Nat. Photonics **4**, 822 (2010).
[53] A. Rundquist, C. G. Durfee, Z. Chang, C. Herne, S. Backus, M. M. Murnane, and H. C. Kapteyn, Science **280**, 1412 (1998).
[54] D. D. Hickstein, P. Ranitovic, S. Witte, X.-M. Tong, Y. Huismans, P. Arpin, X. Zhou, K. E. Keister, C. W. Hogle, B. Zhang, C. Ding, P. Johnsson, N. Toshima, M. J. J. Vrakking, M. M. Murnane, and H. C. Kapteyn, Phys. Rev. Lett. **109**, 073004 (2012).
[55] See Supplemental Material at http://link.aps.org/supplemental/10.1103/PhysRevLett.117.133201 for additional information on the experimental apparatus and the implementation of the CE and CTMC simulations, as well example electron trajectories.
[56] M. V. Ammosov, N. B. Delone, and V. P. Krainov, Zh. Eksp. Teor. Fiz. **91**, 2008 (1986) [Sov. Phys. JETP **64**, 1191 (1986)].
[57] J. P. Paquette and J. L. Chaloupka, Phys. Rev. A **79**, 043410 (2009).
[58] J. L. Chaloupka and D. D. Hickstein, Phys. Rev. Lett. **116**, 143005 (2016).
[59] S. Eckart *et al.*, following Letter, Phys. Rev. Lett. **117**, 133202 (2016).